REVISTA MATÉRIA V.30
ISSN 1517-7076 articles e20250307, 2025

Dual waste valorization in concrete: a performance-based study on waste foundry sand and bottom ash materials

Kiruthika Baskar[1], Arunkumar Ganesan[2], Karthiga Baskar[1]

[1]Paavai Engineering College, Department of Civil Engineering. 637018, Namakkal, India.
[2]Government College of Engineering, Department of Civil Engineering. 636011, Salem, India.
e-mail: kiruthikabaskar1211@gmail.com, arun_81120050@yahoo.com, karthigabaskar5030@gmail.com

ABSTRACT

The rising global demand for sustainable construction materials has catalyzed the exploration of industrial byproducts in concrete production, aiming to reduce environmental impact while maintaining structural integrity. Among these byproducts, WFS and BA are two prominent solid waste streams generated from the metal casting and thermal power sectors, respectively. Their potential as partial replacements for natural fine aggregates in concrete has gained increasing attention due to their availability and environmental benefits. This study evaluates the mechanical and durability performance of concrete with WFS and BA, both as standalone and binary combinations. A total of eleven distinct mix designs were prepared and tested, with replacement levels ranging from 0% to 40%. The optimum blend, consisting of 20% WFS and 20% BA, exhibited significant performance enhancements compared to the control mix. Improvements included a 7.8% increase in 28-day compressive strength, a 7.5% rise in split tensile strength, and a 7.7% boost in flexural strength. Durability parameters also improved notably, with an 18.2% reduction in chloride ion permeability, a 14.5% decrease in drying shrinkage, and an 11.2% limitation in acid-induced strength loss. These findings highlight the synergistic effects of WFS and BA in improving concrete quality, to sustainable waste valorization in construction materials.

Keywords: Waste foundry sand; Bottom ash, sustainable concrete; Durability performance; Fine aggregate replacement.

1. INTRODUCTION

Concrete remains the cornerstone of modern construction, with over 30 billion tonnes consumed annually worldwide. Yet, its widespread use has come at a considerable environmental cost [1]. The manufacture of Portland cement, the primary binding material in concrete, contributes nearly 8% of total global CO_2 emissions, while the extraction of river sand for fine aggregates disrupts ecosystems and depletes natural resources at an unsustainable rate. As the construction industry confronts escalating environmental regulations, resource scarcity, and increasing demand for infrastructure in developing economies, there is a growing consensus that conventional concrete systems must evolve toward more sustainable, circular, and resource-efficient alternatives.

In response to these challenges, researchers and industries are turning to waste valorization as a promising pathway. The current era is witnessing a paradigm shift from disposal-centric waste management toward a circular economy model, wherein industrial byproducts are repurposed into construction materials. Among these, WFS—a byproduct from metal casting—and Bottom Ash (BA)—generated from thermal power plants—have emerged as high-potential substitutes for natural fine aggregates in concrete. These materials are abundantly available, underutilized, and pose environmental hazards if not properly managed. Transforming them into construction inputs [2]

Despite their potential, the integration of WFS and BA into concrete has faced certain limitations. Most studies to date have focused on their individual use, neglecting the possibility of synergistic effects when both materials are blended. Furthermore, existing research tends to emphasize early-age compressive strength while overlooking long-term durability, service life performance, and environmental resistance—parameters crucial to ensure the viability of sustainable concrete under real-world conditions. Without addressing these aspects, the widespread adoption of waste-integrated concrete remains constrained [3].

Corresponding Author: Kiruthika Baskar Received on 06/04/2025 Accepted on 19/08/2025

DOI: https://doi.org/10.1590/1517-7076-RMAT-2025-0307

In addition, a clear research gap exists in the optimization of binary fine aggregate replacements using advanced statistical and AI-based tools. Traditional mix design methods typically involve trial-and-error approaches, which are laborious and fail to account for interaction effects among materials. This lack of precision limits the reproducibility and scalability of findings. In contrast, modern tools such as RSM and machine learning-based regression models enable predictive and optimized mix designs, reducing the experimental workload and yielding scientifically robust outcomes. However, these tools have yet to be widely applied to concrete mixes incorporating combined WFS and BA [4].

Another under-addressed issue in earlier studies is the lack of lifecycle-relevant performance indicators, such as resistance to chloride ingress, capillary absorption, shrinkage, and acid attack. Durability metrics are essential not only for structural safety but also for reducing maintenance costs and embodied carbon over the lifespan of concrete infrastructure. Integrating these tests into the evaluation framework ensures that proposed mixes are not only environmentally friendly at the material level but also perform effectively in harsh environments.

Moreover, while some studies mention the environmental benefits of using industrial wastes, very few substantiate these claims with microstructural validation. Techniques such as SEM and EDS provide insight into the internal morphology and phase distribution of the cement matrix, helping to correlate macro-performance with microstructure. Their inclusion enhances the scientific rigour of any sustainable concrete study, but they are seldom included in investigations involving WFS and BA.

Table 1, highlights extensive research on the use of BA in concrete, either independently or in combination with other materials like fly ash, GGBS, and construction debris. While studies emphasize the mechanical and durability benefits of BA up to optimal replacement levels (typically 20–50%), others explore its synergistic use with other waste materials for performance enhancement [15]. This review highlights the necessity for a more comprehensive approach in assessing the performance of concrete developed with the incorporation of dual industrial waste, particularly in the context of sustainability and circular economy practices.

Addressing these gaps, the present research investigates the innovative use of combined WFS and BA as fine aggregate replacements in concrete, providing a practical and high-impact solution that aligns with global sustainability and waste management trends. Unlike previous studies, this work does not evaluate these materials in isolation but explores their binary synergy, aiming to harness the best attributes of both—WFS's fine texture for improved packing density, and BA's pozzolanic nature for enhanced durability [16].

An additional innovation of this study is its application of RSM for optimizing the replacement levels of WFS and BA. RSM enables the development of statistically validated predictive models that assess the individual and interactive effects of WFS and BA on key performance parameters. Optimization through RSM not only ensures efficient material use but also identifies ideal combinations that balance sustainability with mechanical and durability performance [17].

To further enrich the experimental findings, advanced microstructural analysis using SEM/EDS has been incorporated to assess the morphological evolution of the cement matrix resulting from the addition of WFS and BA. This provides visual and elemental confirmation of hydration product development, pore refinement, and interface transitions, thereby explaining observed improvements or declines in macro-scale performance. Such comprehensive characterization is vital for the development of next-generation concrete technologies that are both sustainable and technically viable [18].

The novelty of this research lies in its multi-criteria approach—evaluating mechanical, durability, and microstructural properties simultaneously while optimizing WFS and BA levels using advanced statistical tools. This is complemented by using comparison metrics from recent literature to benchmark performance [19]. The inclusion of a Taylor diagram and radar chart for visual analysis further enhances the clarity of multi-variable performance assessments, making it easier for engineers and researchers to identify the most effective mix combinations [20].

By aligning with cutting-edge trends in green construction and digital optimization, this study makes a meaningful contribution to the global discourse on sustainable concrete design. It not only provides experimental evidence for the responsible reuse of industrial byproducts but also delivers a predictive framework for material selection and proportioning—paving the way for data-driven, low-carbon concrete solutions. This is particularly relevant for developing nations where industrial waste is abundant and construction growth is rapid, making the findings of this study both timely and globally scalable [21].

This research tackles one of the most pressing challenges in civil engineering today: how to make concrete more sustainable without compromising performance [22]. By exploring the combined use, integrating lifecycle durability assessments, optimizing material combinations using RSM, and validating results through

Table 1: Summary of BA and related industrial byproducts in concrete.

FOCUS AREA	MATERIALS USED	KEY FINDINGS	RELEVANCE TO CURRENT STUDY
ANN prediction of strength	Fly ash, Bottom ash	Bayesian ANN model successfully predicts compressive strength	It predicts strength using BA and fly ash via AI and supports performance modeling,ut does not explore physical blending [5].
Mechanical & durability using GCBA and CBA as binder & fine aggregate	GCBA, CBA	Optimum: 21.8% GCBA + 24.17% CBA; reduced CO_2 and cost	Demonstrates dual usage, supporting comparisons of pozzolanic reactivity and mechanical durabilityelevant to BA use [6].
Soil remediation using BA-based geopolymer and coir	Bottom ash, Coir	10% geopolymer solidified 95% of heavy metals in soil	Focuses on soil remediation, offering insight into the reuse of BA,ut not in concrete matrix systems [7].
Cement concrete	Bottom ash	BA up to 40% improves strength and durability	Directly supports BA as a fine aggregate; aligns with your findings on mechanical and durability performance [8].
BA as fine aggregate in GGBS-based geopolymer concrete	Bottom ash, GGBS	20–40% BA showed good strength, acid and sulfate resistance	Explores BA in geopolymer; provides a useful comparison to your OPC system, although the type of binderiffers [9].
Optimum CBA/CBS for sustainable concrete	CBA, CBS	50% CBA/CBS optimized; CBA outperforms CBS in compressive strength	Highly relevant to optimization and strength findings of BA, especially regarding environmental benefits [10].
Environmental and chemical analysis of coal ash concrete	Fly ash, Bottom ash	No heavy metal leaching; FA & BA are safe and sustainable replacements	Reinforces environmental safety of BA, supporting your sustainability claims [11].
Concrete with FA, BA, GGBS, construction debris	BA, FA, GGBS	15% GGBS and up to 20% BA improved mechanical properties	Aligns with your goal of blending waste materials to enhance performance and conserve resources [12].
Use of SCBA and CBA in concrete	SCBA, CBA	10% SCBA + 10% CBA yielded better strength and workability	It strongly supports the blended use of industrial waste; the findings directly align with the benefits of your WFS+BA combined mix [13].
Effect of FA & BA in fiber-reinforced concrete	Fly ash, Bottom ash, Fibers	30% FA/BA optimal for GFRC; 20% for PPFrc; good strength & low shrinkage	Provides useful insights into durability and shrinkage when BA is combined with other components, such asibers [14].

advanced microstructural techniques, the study offers a comprehensive and forward-looking solution. It reflects a shift away from incremental improvements in traditional materials toward innovative, systemic approaches that embrace waste reuse, performance optimization, and environmental responsibility [23].

The primary objective of this study is to develop and optimize a concrete mix incorporating WFS and BA as partial replacements for fine aggregate, achieving desirable mechanical strength and superior durability properties while significantly reducing reliance on natural sand. This will be achieved through extensive laboratory experimentation, statistical optimization via Response Surface Methodology, and microstructural analysis using SEM/EDS. Through this multifaceted approach, the research aims to establish a technically sound and environmentally responsible concrete system that can serve as a model for future material innovations in the construction industry.

2. MATERIALS AND METHODS

This study compared the impact of WFS, BA, and their combinations on the strength and durability of concrete. Experiments included material characterization, concrete mix design, specimen casting and curing, and tests for mechanical and durability properties. The WFS utilized in the study was obtained from a local ferrous casting facility. It was dark grey in color and exhibited fine, angular particles. The sand was dried, sieved through a 4.75 mm sieve, and stored in sealed containers to prevent moisture absorption. Characterization using (EDS) revealed that WFS consisted primarily of silica (>80%) along with trace amounts of iron, aluminum, and other

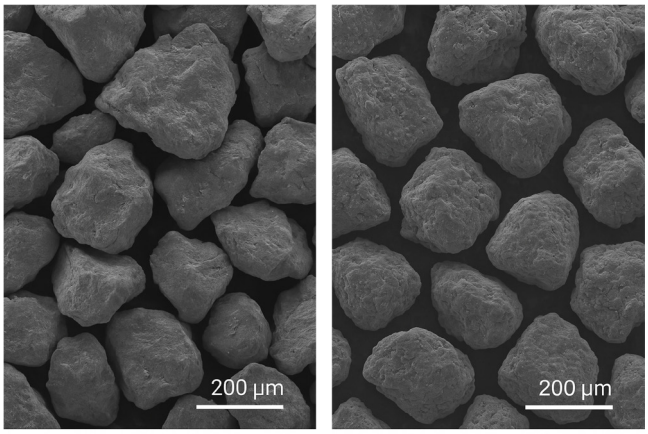

Figure 1: SEM micrographs of (a) and (b) showing surface texture and particle morphology.

metal oxides. The mineralogical phases of BA were identified through XRD, indicating the presence of quartz and mullite, while its chemical composition obtained via XRF included 55% SiO_2, 20% Al_2O_3, and 10% Fe_2O_3. In addition to their basic physical characteristics, a more detailed understanding of the properties of WFS and BA is crucial for assessing their compatibility with cementitious systems. The particle size distribution of WFS was found to be skewed toward the finer range, with 90% of particles passing through a 150 µm sieve, which contributes to its filler effect and enhances particle packing. Its bulk density was recorded at approximately 1.6 g/cm^3, and its water absorption capacity was relatively low at 1.2%, indicating limited porosity. On the other hand, BA exhibited a broader particle size range and a more irregular shape, with a bulk density of 1.3 g/cm^3 and a water absorption value of 4.8%, highlighting its porous and absorptive nature. The pozzolanic activity index of BA, determined by ASTM C618, was measured at 72% after 28 days, confirming its potential to contribute to secondary hydration. Additionally, the loss on ignition (LOI) for WFS and BA was found to be below 3%, suggesting minimal presence of unburnt carbon or organic impurities. These additional properties play a crucial role in understanding the behavior of these materials within the cement matrix, particularly in terms of workability, water demand, and long-term durability. Scanning electron micrographs depicting the particle morphology of WFS and BA are presented in Figure 1.

SEM images revealed denser and more homogeneous matrices in mixes containing WFS and BA, indicating improved packing and reduced pore interconnectivity, which aligns with the lower sorptivity and water absorption results. XRD patterns showed diminished peaks of portlandite and an increased formation of amorphous phases, reflecting the consumption of calcium hydroxide through pozzolanic activity—an effect known to enhance chemical stability and reduce vulnerability to leaching. Additionally, TGA analysis indicated a lower weight loss in the range associated with $Ca(OH)_2$ decomposition in modified mixes, corroborating the reduced permeability and higher resistance to chemical degradation. Collectively, these microstructural features validate the improved durability behavior observed in experimental tests and demonstrate that the inclusion of WFS and BA not only enhances physical resistance but also fundamentally alters the internal structure to mitigate shrinkage and permeability-related failures [24].

The mixing water used in all concrete batches conformed to IS 456:2000 standards. No chemical admixtures were employed to isolate and independently study the influence of WFS and BA. To account for the influence of aggregate moisture on mix consistency, the moisture content of fine and coarse aggregates, including WFS and BA, was measured prior to batching using the oven-drying method as specified in IS 2386 (Part 3): 1963. Samples were dried at 105 ± 5 °C for 24 hours, and the difference in weight was used to calculate moisture percentage. These values were used to correct the net mixing water to maintain a constant effective water-to-cement ratio across all batches. WFS, owing to its finer particle size and higher surface area, exhibited slightly higher moisture retention compared to natural sand. Bottom ash, being more porous and angular, also showed variability depending on ambient humidity. These differences were addressed by adjusting the volume of added water accordingly during the mixing stage. This correction was vital to ensure uniform workability and accurate comparison of mechanical and durability properties. Without such adjustments, water variability could have led to inconsistent strength development or misinterpretation of the influence of the waste materials. The replacement was performed by weight, and all other parameters, including cement content, water-to-cement ratio, and aggregate proportions, were kept constant [25].

Figure 2: Experimental methods in this work.

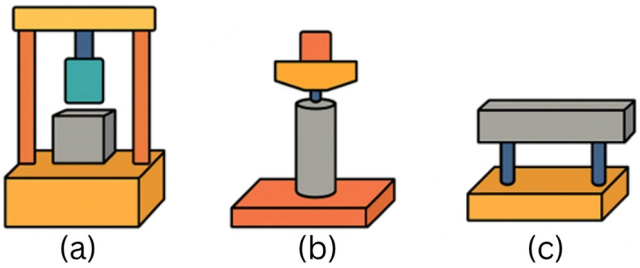

Figure 3: Mechanical testing setup (a) Compression testing machine with cube (b) Split tensile setup with cylinder (c) Flexural testing on third-point loading setup.

Figure 2 illustrates the experimental setup used for concrete mixing, evaluation of fresh properties, and specimen casting. The process begins with the use of a pan mixer, which is employed to ensure uniform mixing of the dry components (cement, aggregates, WFS/BA), followed by the gradual addition of water. The mixer allowed homogeneous blending, minimizing the formation of agglomerates, particularly important when fine additives like (WFS) were used [26]. A digital weighing balance ensured accurate proportioning of materials according to mix design ratios, batching cement, aggregates, WFS, BA, and water by mass. This precision was crucial for achieving uniformity in trial batches and ensuring the reproducibility of results. The slump value indicated consistency, influenced by WFS angularity and BA's internal water retention. The concrete was then transferred to molds, compacted with a table vibrator, and lightly oiled to ensure smooth demolding, thereby achievg consistent geometry and surface finish for reliable mechanical and durability tests [27].

Figure 3 illustrates the mechanical testing setups for evaluating concrete mixes with (WFS), (BA), and their combinations. Three tests were conducted, following the IS codes. The compressive strength test used a compression testing machine, as per IS 516:1959. Load was applied gradually until failure to assess load-bearing capacity, shown in the Figure 3(a) [28]. Figure (b) depicts this setup, which is important for understanding brittleness and crack resistance under indirect tension. The flexural strength test utilized prismatic beams that were supported at their ends and loaded at one-third of their spans using a flexural testing frame, as per IS 516:1959. Figure (c) illustrates this arrangement, which is crucial for evaluating concrete's bending stress resistance inavement and slab applications [29].

Figure 4 illustrates the types of concrete specimens prepared and tested in this study, along with their respective dimensions and intended purpose. To ensure a comprehensive evaluation of mechanical and durability characteristics, four standard specimen types were cast for each concrete mix [30]. This standardized curing environment ensured consistent hydration and strength development across all specimens [31]. All cast specimens were subjected to standard water curing to ensure consistent hydration and strength development. After demolding at 24 ± 2 hours, the samples were fully immersed in a curing tank containing clean tap water maintained at a temperature of 27 ± 2°C, in accordance with IS 516:2018. This curing condition was selected to eliminate environmental variability and to provide sufficient moisture for the complete hydration of cementitious materials, especially critical when supplementary materials such as WFS and BA are used. Uniform curing practices across all mix types ensured that observed differences in performance could be attributed to mix composition rather than curing variability. Additionally, temperature and water levels in the curing tank were monitored regularly to maintain consistent curing conditions throughout the study.

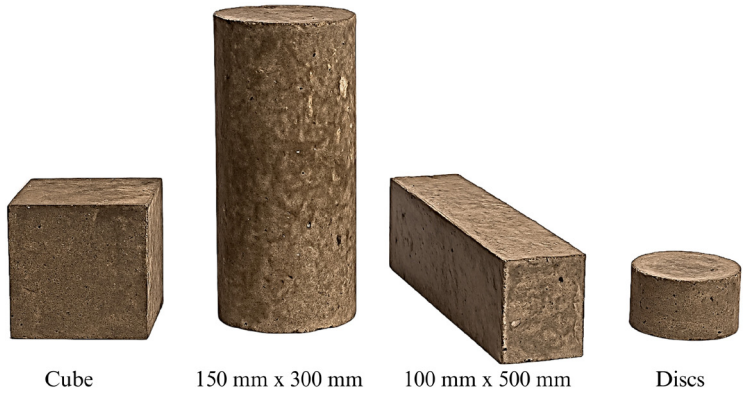

Figure 4: Prepared samples.

Mix ID	WFS (%)	BA (%)	Compressive	Split Tensile	Flexural
CTRL	0	0	✓	✓	✓
WFS10	10	0	✓	✓	✓
WFS20	20	0	✓	✓	✓
WFS30	30	0	✓	✓	✓
WFS40	40	0	✓	✓	✓
BA10	0	10	✓	✓	✓
BA20	0	20	✓	✓	✓
BA30	0	30	✓	✓	✓
BA40	0	40	✓	✓	✓
WFS10+BA10	10	10	✓	✓	✓
WFS20+BA20	20	20	✓	✓	✓

Figure 5: Mix designation and testing matrix used to assess mechanical properties of concrete.

This specimen preparation strategy enabled a multi-angle evaluation of how the inclusion of (WFS), (BA), and their combinations influenced both early and long-term concrete performance [32]. After ensuring uniform mixing, the fresh concrete was evaluated for its workability using the standard slump cone method as per IS 1199:1959. This test was deemed necessary, especially since no superplasticizers or chemical admixtures were incorporated into the mix, which could otherwise influence workability. Slump measurements were recorded for all mixes, including control, WFS-only, BA-only, and combined WFS–BA variants. It was observed that the slump values ranged between 48 mm and 70 mm across all trials, indicating a workable mix suitable for placement and compaction by conventional methods. Slight reductions in workability were observed with increasing WFS content, attributed to its angular particle morphology and higher surface area, which increased internal friction and water demand. Conversely, the inclusion of BA helped retain workability due to its spherical particles and glassy surface texture, which improved flow characteristics. The slump test confirmed that all designed concrete blends maintained adequate workability for practical applications, even in the absence of admixtures [33]. The experimental matrix used for mechanical testing is illustrated in Figure 5.

Durability tests included water absorption, sorptivity, RCPT, sulfate and acid resistance, and drying shrinkage. Water absorption was measured as per ASTM C642 by oven-drying samples at 105°C for 24 hours, followed by 24-hour water immersion to determine mass gain. Sorptivity was evaluated using 100 mm × 50 mm cylindrical specimens partially immersed in water, with cumulative absorption measured over time and the sorptivity index derived from the initial linear portion of the absorption vs. √time plot, following IS 516 (Part 5, Sec 1): 2018. All specimens underwent 28 days of water curing, oven-drying, and desiccation prior to testing. The RCPT test (ASTM C1202) assessed chloride ion permeability by applying 60 V across 50 mm concrete discs for 6 hours, with total charge passed used for classification [34]. The control mix exhibited 3345 coulombs (moderate permeability), while the 20% WFS + 20% BA blend showed 1798 coulombs (low permeability),

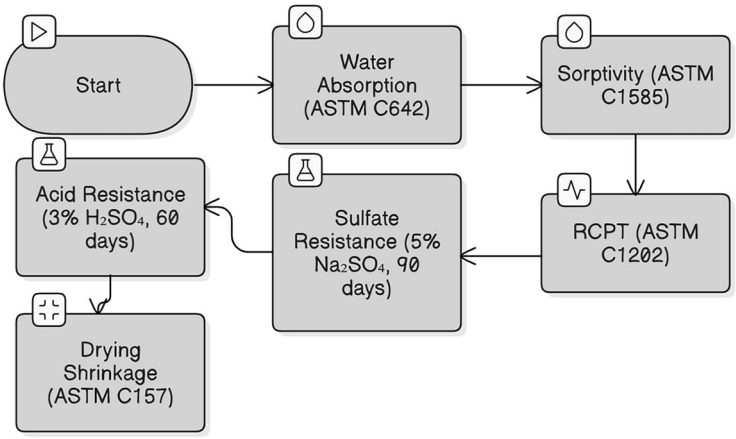

Figure 6: Flowchart of the testing procedure.

indicating a 46.3% reduction. This improvement is attributed to microstructural densification and pozzolanic activity from the additives. Sulfate resistance was evaluated by immersing cubes in 5% Na_2SO_4 for 90 days, and acid resistance was assessed by 60-day exposure to 3% H_2SO_4, with strength loss calculated post-exposure. Drying shrinkage was monitored on prism specimens per ASTM C157. These tests collectively confirmed that binary mixes improved durability by minimizing ionic transport, enhancing chemical resistance, and reducing shrinkage-related degradation. A summary of the durability evaluation sequence and methods used is shown in Figure 6.

Microstructural analysis, including SEM and EDS, was performed on control and various WFS and BA mix specimens to understand material behavior. These analyses examined hydration products, porosity, and interfacial bonding. All tests were performed in triplicate, with standard deviations recorded to ensure statistical reliability, thereby providing a detailed comparison of the effects of WFS, BA, and their combinations on concrete performance [35].

To ensure the reliability and reproducibility of experimental findings, all mechanical and durability tests were conducted in triplicate, and the average values were reported. The use of multiple specimens for each test condition enabled statistical comparison and helped minimize anomalies caused by equipment variation, material inconsistencies, or human error. For each property three specimens were cast and tested as per relevant IS codes. The resulting standard deviations for most properties remained within acceptable ranges (typically less than 5% of the mean), confirming the consistency of the results. The inclusion of statistical measures also enabled better interpretation of trends across replacement levels, particularly in cases where marginal differences in performance were observed. This approach provided robust evidence of the observed improvements or reductions in performance, thereby strengthening the validity of the study's conclusions.

3. RESULTS AND DISCUSSION

The findings revealed distinct patterns in strength performance, workability variation, and resistance to environmental degradation, which are elaborated upon in the subsequent sections.

The slump test assessed concrete workability, showing decreased values with higher WFS content. Figure 7 shows the variation in slump incorporating WFS, BA, and their binary combinations. With the increase in WFS content, slump values decreased progressively from 75 mm (control) to 49 mm at 40% replacement, indicating a 34.7% reduction [36]. The 10% and 20% WFS mixes exhibited slumps of 68 mm and 62 mm, representing reductions of 9.3% and 17.3%, respectively, while the 30% WFS mix experienced a 24% slump loss. These trends suggest that WFS hinders paste mobility at higher volumes due to particle shape and insufficient water for lubrication [37]. Conversely, mixes incorporating BA demonstrated a consistent increase in slump values with increasing replacement levels. At 10%, 20%, 30%, and 40% BA, the slump improved to 81 mm, 85 mm, 89 mm, and 94 mm, reflecting respective increases of 8%, 13.3%, 18.7%, and 25.3% over the control [38]. Combination mixes (10% WFS + 10% BA and 20% WFS + 20% BA) yielded intermediate slump values of 70 mm and 74 mm, only slightly below the control. These values reflect the balancing effect of the two materials, where BA's lubricating benefits counteract WFS's frictional drawback king combination mixes ideal when both sustainability and acceptable workability are desired [39].

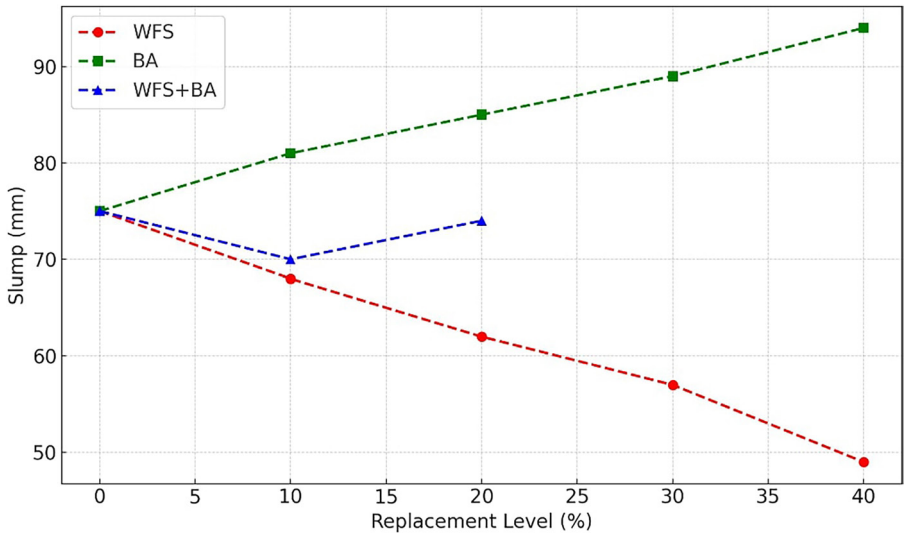

Figure 7: Variation in slump values for concrete mixes containing WFS, BA, and their combinations.

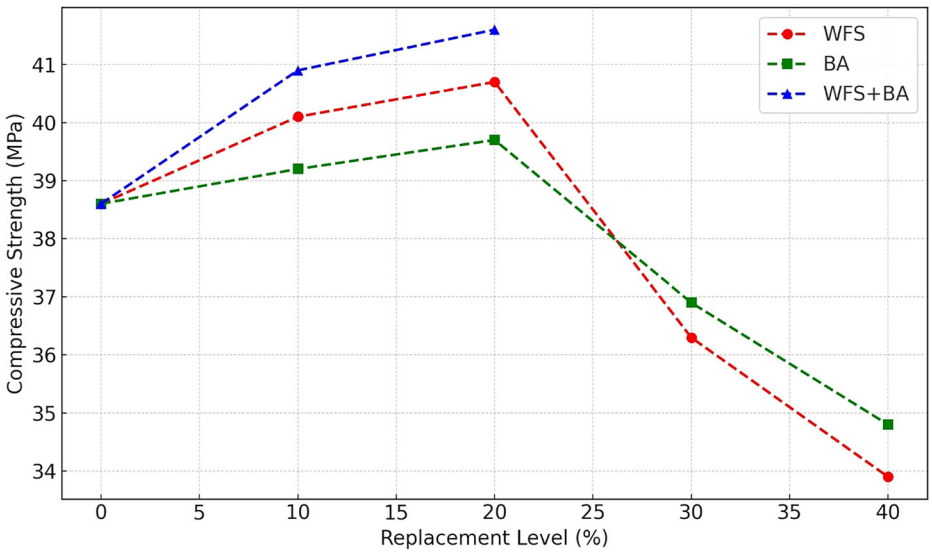

Figure 8: 28-day compressive strength of concrete mixes with varying levels of WFS, BA, and their combinations.

Figure 8 shows the varying percentages of (WFS), (BA), and their binary combinations. This reveals how replacement of natural sand with these materials impacts compressive performance due to their distinct physical and chemical characteristics [40]. For the WFS series, a noticeable increase in strength. The compressive strength improved from 38.6 MPa (control) to 40.1 MPa and 40.7 MPa at 10% and 20% WFS, representing gains of approximately 3.9% and 5.4%, respectively. These improvements can be attributed to the filler effect of the finer WFS particles, which helped densify the matrix at lower contents. However, strength declined to 36.3 MPa (−6.0%) at 30% WFS and to 33.9 MPa (−12.2%) at 40% WFS. This reduction was likely due to poor particle packing, increased voids, and higher water demand resulting from the high surface area and angular shape of WFS, which led to a weaker microstructure.

The trend for BA mixes followed a similar but milder pattern. Strength peaked at 20% BA with 39.7 MPa, a 2.8% increase over the control, due to moderate pozzolanic activity and better water retention. However, a decline to 36.9 MPa and 34.8 MPa at 30% and 40% BA indicated that excessive BA content diluted the cementitious matrix and introduced excessive porosity [41]. Combination mixes demonstrated the best performance. The 10% WFS + 10% BA mix reached 40.9 MPa, a 6.0% improvement, while the 20% + 20% blend achieved 41.6 MPa—a 7.8% increase. These results suggest a synergistic interaction where BA's pozzolanic

action and porous structure counterbalance WFS's drawbacks, leading to improved hydration and matrix continuity. Thus, the optimal balance in the combined mix yielded superior strength, making the blend a viable solution for enhancing sustainability without compromising mechanical integrity.

Figure 9 presents a bar chart comparison of the 7 & 28-day compressive strengths for concrete mixes containing varying proportions of WFS, BA, and their binary blends. The control mix attained 27.5 MPa at 7 days and 38.6 MPa at 28 days. Upon replacing natural sand with 10% and 20% WFS, the 28-day strength improved to 40.1 MPa and 40.7 MPa, representing increases of 3.9% and 5.4%, respectively. The enhancement is attributed to the filler effect of fine WFS particles, which increase packing density and reduce voids at moderate dosages. However, at 30% and 40% WFS, the strength declined to 36.3 MPa (−6%) and 33.9 MPa (−12.2%), respectively, due to the increased surface area and angularity, which elevated water demand and reduced cohesion in the matrix. In the case of BA, 10% and 20% replacements yielded 39.0 MPa and 39.7 MPa, respectively, improving the strength by 1.0% and 2.8% over the control. The porous nature of BA enables internal curing and pozzolanic reactivity, thereby enhancing early hydration. However, excessive BA (30% and 40%) diluted the cementitious phase, resulting in a drop in strength to 37.0 MPa and 34.8 MPa. Notably, the binary blends (WFS10+BA10 and WFS20+BA20) outperformed all individual substitutions, achieving 40.9 MPa and 41.6 MPa at 28 days. The trend confirms that dual replacement optimally balances mechanical performance with sustainability goals (Table 2).

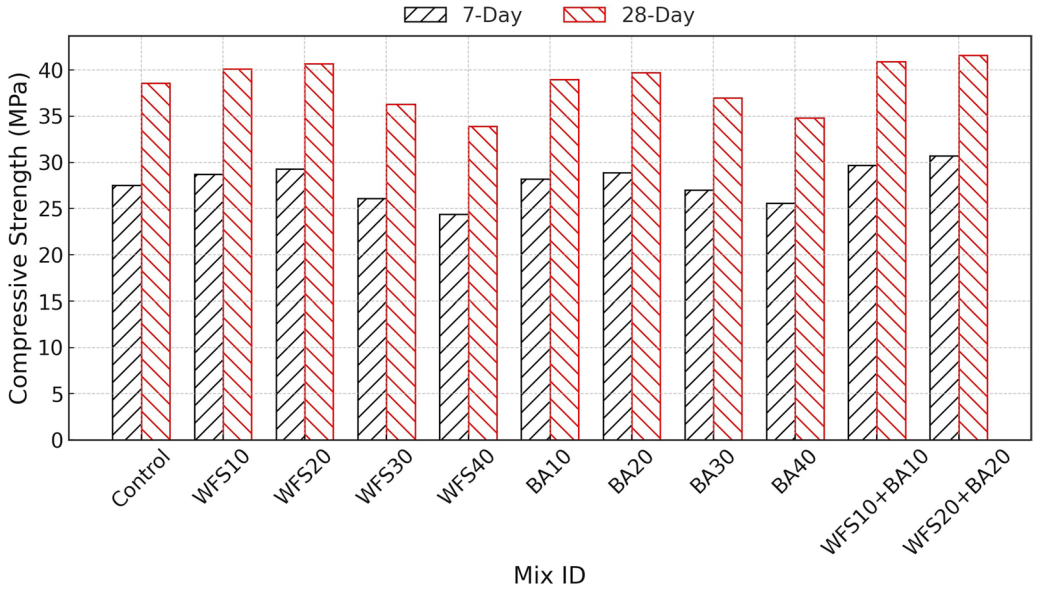

Figure 9: Comparison of 7 & 28-day compressive strengths for concrete mixes.

Table 2: Statistical analysis of 28-Day compressive strength.

MIX ID	MEAN (MPa)	STANDARD DEVIATION	MINIMUM (MPa)	MAXIMUM (MPa)	COEFFICIENT OF VARIATION (%)
Control	38.60	0.10	38.50	38.70	0.26
WFS10	40.10	0.10	40.00	40.20	0.25
WFS20	40.70	0.10	40.60	40.80	0.25
WFS30	36.30	0.10	36.20	36.40	0.28
WFS40	33.90	0.10	33.80	34.00	0.29
BA10	39.00	0.10	38.90	39.10	0.26
BA20	39.70	0.10	39.60	39.80	0.25
BA30	37.00	0.15	36.80	37.10	0.41
BA40	34.80	0.10	34.70	34.90	0.29
WFS10+BA10	40.90	0.10	40.80	41.00	0.24
WFS20+BA20	41.60	0.10	41.50	41.70	0.24

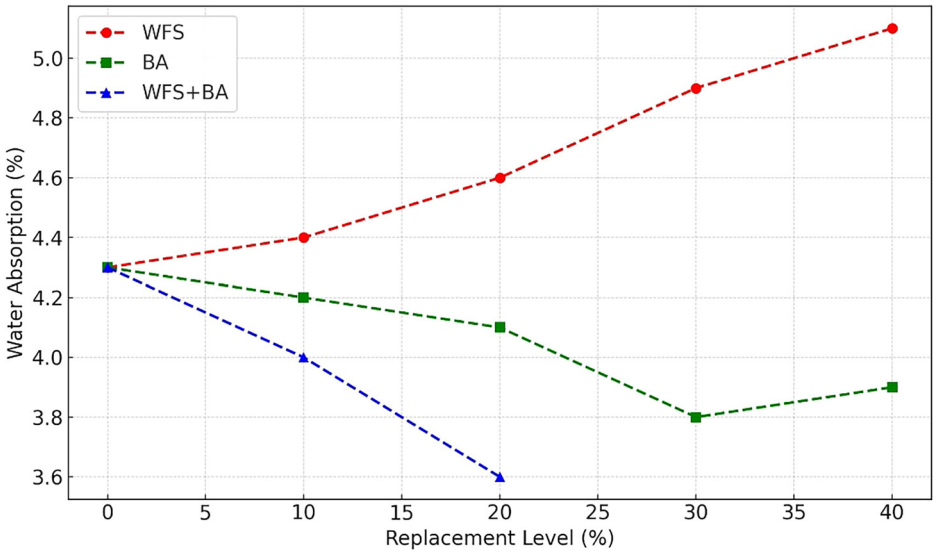

Figure 10: Split tensile and flexural strength performance of WFS, BA, and blended mixes.

Figure 10 illustrates the variation in split tensile and flexural strength of concrete with different replacement levels of (WFS), (BA), and their binary combinations [42]. In the split tensile strength results, the control mix yielded a tensile strength of 3.45 MPa. For WFS-replaced mixes, strength improved slightly at lower replacement levels, reaching 3.52 MPa and 3.58 MPa at 10% and 20% WFS, respectively. BA mixes displayed a similar but slightly more favourable trend. Split tensile strength increased modestly to 3.54 MPa at 20% BA (a 2.6% improvement), then reduced to 3.38 MPa and 3.25 MPa at 30% and 40% replacements, respectively. The superior performance at 20% BA is attributed to moderate pozzolanic reactivity and improved water retention properties, which enhance bond development and reduce shrinkage cracking. Combination mixes exhibited the highest split tensile strengths. The 10% WFS + 10% BA mix reached 3.63 MPa (5.2% increase), while the 20% + 20% blend peaked at 3.71 MPa, a 7.5% improvement. These enhancements suggest synergistic effects where BA offsets WFS-induced brittleness by improving matrix cohesion, internal curing, and shrinkage resistance [43]. In the case of flexural strength, the control mix achieved 5.55 MPa. The binary blends showed excellent improvement, with 10% WFS + 10% BA resulting in 5.80 MPa and 20% + 20% achieving the maximum value of 5.98 MPa—an increase of 7.7% over the control. This reflects enhanced tensile stress distribution and crack-bridging facilitated by denser microstructures and improved aggregate-paste interaction in the blended mixes. The results reinforce that WFS and BA, when used together, can significantly enhance tensile-related properties of concrete, especially at balanced substitution levels.

Figure 11 shows the water absorption behavior of concrete mixes containing varying percentages of (WFS), (BA), and their combinations. The data clearly reflect the influence of particle morphology, pozzolanic reactivity, and packing density on the permeability characteristics of hardened concrete [44]. The control mix exhibited a water absorption rate of 4.3%. With the inclusion of WFS, a steady increase in absorption was observed: 4.4% at 10% replacement, rising to 5.1% at 40% WFS, which corresponds to an 18.6% increase compared to the control. These voids create preferential pathways for water ingress, thus elevating permeability [45]. In contrast, the BA mixes demonstrated significantly improved performance. At 10% and 20% BA, the water absorption reduced to 4.2% and 4.1%, respectively, while the lowest value of 3.8% was recorded at 30% BA—an 11.6% decrease relative to the control. This improvement is mainly due to the porous nature of BA, which initially absorbs and later releases water, acting as an internal curing agent [46]. Mixes with 10% WFS + 10% BA and 20% WFS + 20% BA showed the best performance, absorbing 4.0% and 3.6% water, respectively. The 3.6% rate is 16.3% lower than the control, indicating that combining WFS and BA compensates for their individual drawbacks. WFS improves packing due to its fine size, while BA enhances matrix densification through pozzolanic activity and internal curing. This combination results in lower permeability and higher durability, making blended WFS-BA mixes ideal for water-resistant applications [47].

Figure 12 shows the sorptivity and RCPT results for concrete with WFS, BA, and their blends. These indicators assess concrete durability against water ingress and chloride ion penetration. The control mix had a sorptivity of 0.125 mm/√min. Adding WFS increased values: 0.135 mm/√min at 10% WFS and 0.155 mm/√min

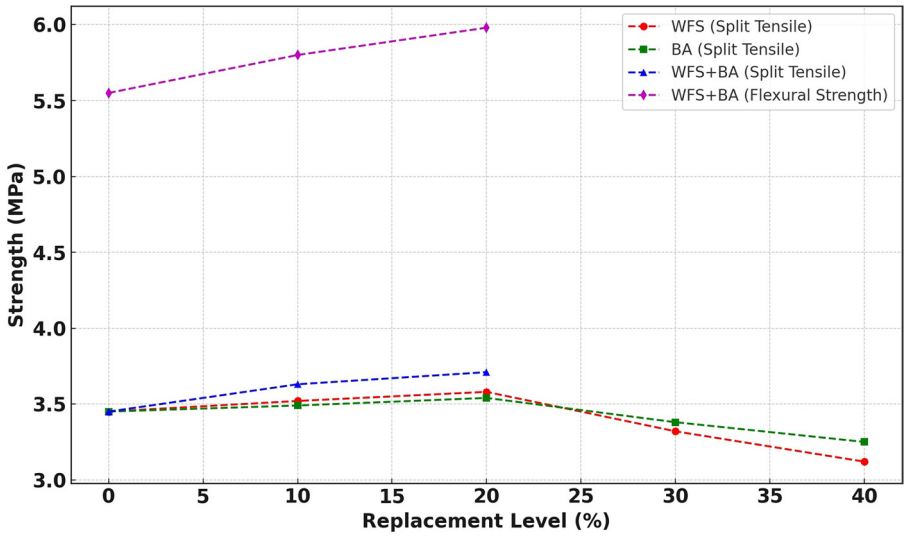

Figure 11: Water absorption rates for concrete incorporating WFS, BA, and their blends.

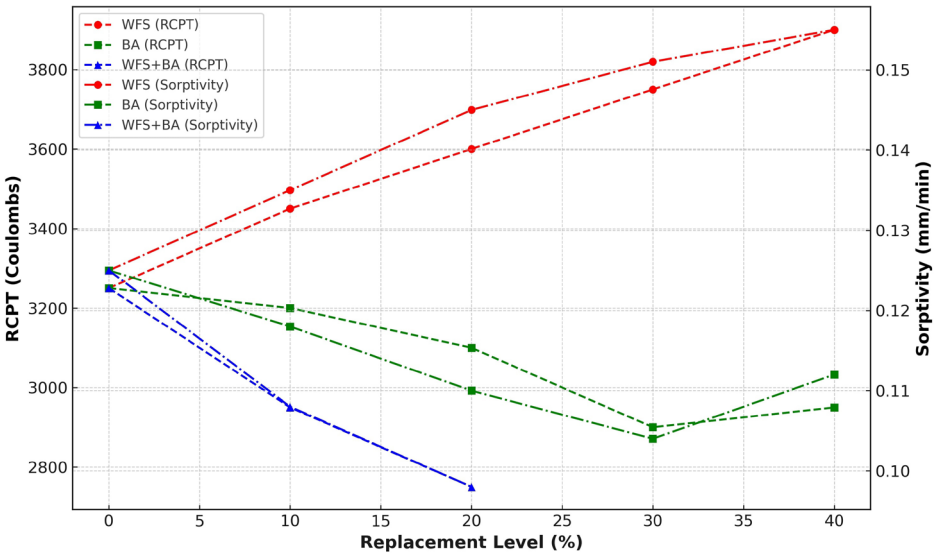

Figure 12: RCPT values for chloride ion permeability of all mixes.

at 40%, a 24% rise. This indicates more capillary pores due to WFS's finer particles and lack of pozzolanic reactivity, reducing the matrix's ability to seal voids during hydration. Additionally, poor bonding at the aggregate-paste interface may have enhanced capillary action [48]. BA mixes, in contrast, showed a steady decline in sorptivity values. At 20% and 30% replacement, values decreased to 0.110 mm/min and 0.105 mm/√min, respectively, reflecting reductions of 12% and 16% compared to the control. This was due to BA's pozzolanic behavior and porous nature, which allowed for better internal curing, leading to a more continuous and refined microstructure. Notably, the 20% WFS + 20% BA combination mix recorded the lowest sorptivity at 0.096 mm/√min—a 23.2% improvement over the control. This highlights the synergy where WFS aids in matrix densification through micro-filling, while BA chemically enhances the binder phase.

The RCPT values followed similar patterns. The control mix recorded 3300 coulombs, categorized under moderate permeability. WFS replacements increased charge passage, reaching 3900 coulombs at 40% WFS—a 18.2% increase—due to increased pore connectivity and reduced continuity of the cementitious matrix. Meanwhile, BA significantly improved resistance, with values dropping to 3100 and 2900 coulombs at 20% and 30% replacement, respectively, corresponding to reductions of 6.1% and 12.1%. This decrease was attributed to BA's pozzolanic action, which forms additional C-S-H gel that refines pores and blocks ion pathways [49].

The 20% WFS + 20% BA mix showed superior chloride resistance, recording just 2700 coulombs—a substantial 18.2% reduction from the control. This finding confirms the densification and durability benefits gained from hybrid replacement, as the combined effects of micro-filling (WFS) and pozzolanic sealing (BA) act in tandem to reduce permeability. These results indicate that the binary WFS-BA blend is a promising solution for durable concrete in aggressive environments.

Exposure to sulfate solution over 90 days revealed significant differences in durability. The control mix experienced a 5.2% weight loss, while 40% WFS mix showed 6.9% loss. BA mixes performed better, with the 20% and 30% BA mixes recording only 4.1% and 3.7% weight loss, respectively. Combination mixes again outperformed individual constituents; the 20% WFS + 20% BA mix exhibited only 3.3% weight loss, reflecting improved chemical resistance [50].

Acid resistance testing involved immersing specimens in 3% H_2SO_4 solution for 60 days. The control mix lost 16.3% of its compressive strength. WFS mixes showed higher deterioration, with 40% WFS leading to a 21.4% strength loss. However, BA mixes demonstrated greater stability, with only a 12.6% loss at a 30% replacement rate. The best performance was achieved by the 20% WFS + 20% BA mix, with a strength loss of just 11.2%, suggesting that the filler effect of WFS and the pozzolanic activity of BA together contribute to reduced acid penetration. The selection of a 3% sulfuric acid (H_2SO_4) concentration and a 60-day immersion duration for the acid resistance test was based on literature precedence and practical relevance, aiming to simulate moderately aggressive environments such as sewer systems, industrial discharge zones, and acidic soil conditions. Previous studies (e.g., IS 516 Part 5/Sec 1: 2018 and related durability literature) have reported that a 3% acid concentration provides a meaningful yet controlled degradation rate, allowing for measurable performance differentiation among concrete mixes within a manageable test period. The 60-day exposure was selected to strike a balance between accelerated degradation and long-term resistance evaluation. Prolonged exposure over two months enables sufficient interaction between the acidic medium and cementitious matrix, particularly for assessing mass loss, surface deterioration, and strength degradation. Moreover, using a consistent concentration and duration across all mixes ensured that observed performance changes were due to mix composition rather than testing inconsistency. The selected protocol thus provides a realistic yet rigorous method for assessing the acid resistance of blended concretes incorporating WFS and BA, aligning with typical durations used in durability assessment studies of a similar scope.

Drying shrinkage was monitored over a period of 90 days. The control mix showed 420 microstrain. WFS mixes exhibited increased shrinkage, reaching 475 microstrain at a 40% WFS content. BA exhibited reduced shrinkage, with the 30% BA mix recording a microstrain of 395. The combination mix of 20% WFS + 20% BA demonstrated the lowest shrinkage at 382 microstrain, suggesting an optimized balance between fineness-induced shrinkage (WFS) and shrinkage mitigation due to internal curing and porosity moderation by BA [51].

To comprehensively understand the combined effect of WFS and BA on the compressive strength of concrete, a RSM-based analytical approach was adopted. The purpose was to model the strength behavior as a function of two independent variables—WFS and BA replacement levels—treated as continuous quantitative factors. Experimental data were collected for eleven distinct mix designs, including various proportions of WFS-only, BA-only, and blended WFS–BA combinations. Since the experimental matrix included both symmetric (e.g., 10%, 20%, 30%, 40%) and hybrid blend points (e.g., 10% WFS + 10% BA), the data were organized in a grid layout. This model captures linear, quadratic, and interaction effects (WFS × BA), allowing for the detection of nonlinearity and synergistic behavior. The fit of the model was verified through ANOVA, which yielded a highly significant F-statistic of 1784.22 and a p-value < 0.0001, indicating that the variation in compressive strength across mixes was statistically significant. The interaction term (WFS × BA) was especially critical in capturing the peak strength behavior observed at moderate replacement levels (specifically, 20% WFS + 20% BA), which could not have been explained by additive models alone.

This analysis approach not only enables visualization but also facilitates prediction and optimization. The curvature of the response confirms the existence of a global maximum within the practical range of replacements, providing quantitative support for mix design decisions. By establishing a robust statistical model and validating it through inferential tests, the response surface analysis enhances the reliability and applicability of the experimental findings for sustainable concrete development.

Figure 13 illustrates the response surface plot showing the combined influence of (WFS) and (BA) replacement levels. The surface was generated using cubic interpolation of experimentally observed data across a matrix of WFS and BA replacements ranging from 0% to 40%. The plot reveals a smooth, nonlinear relationship, with compressive strength peaking at moderate replacement levels and diminishing at higher percentages of individual or combined substitutions. Specifically, this mix achieved a peak strength of 41.6 MPa, approximately 7.8% higher than the control mix (38.6 MPa). The upward slope of the surface from the origin toward

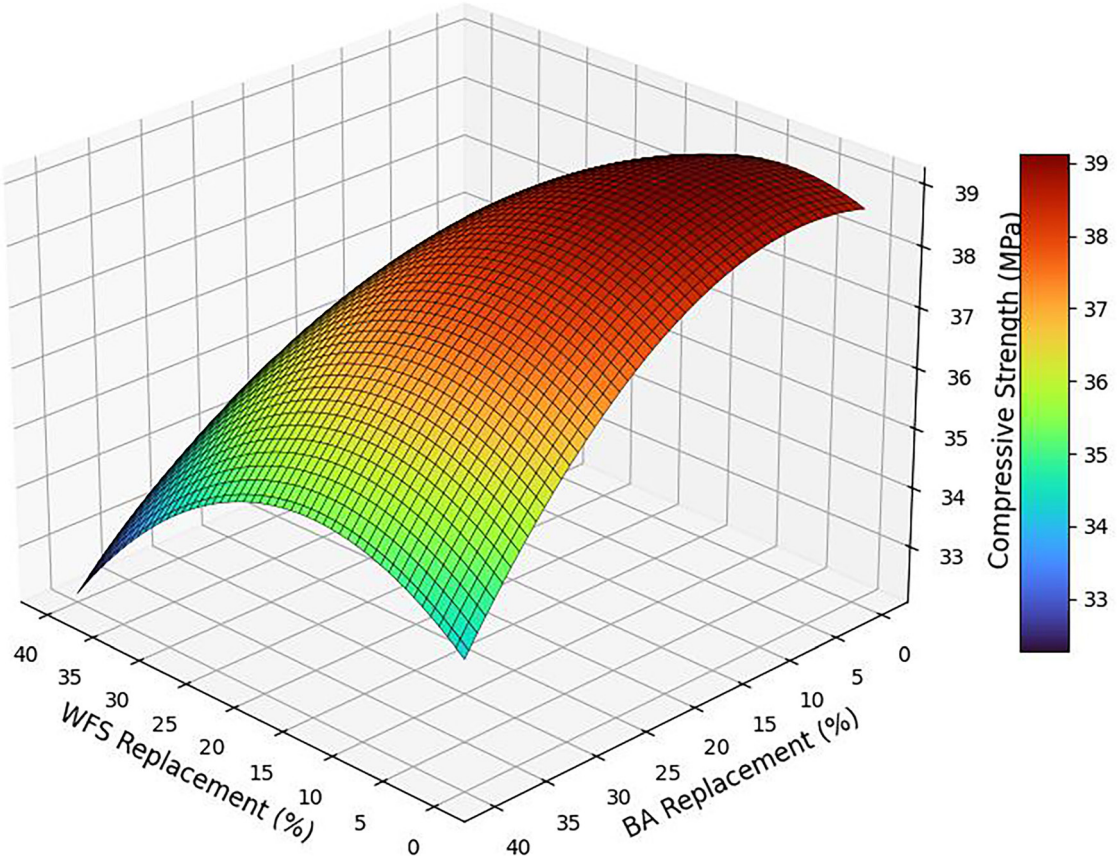

Figure 13: 3d surface plot for compressive strength.

the central zone (20%–25% WFS and BA) indicates a positive interactive effect at lower levels. Conversely, strength declines notably at higher replacement levels (≥30%), with values dipping below the control [52]. This drop-off is attributed to excessive fines from WFS, which increases water demand and porosity, while high volumes of BA may dilute the binder matrix and introduce irregular particle shapes that hinder compaction. The surface curvature illustrates a negative quadratic trend beyond the optimum point, confirming diminishing returns. This validates the ANOVA findings and provides a predictive framework for determining optimal replacement levels. It demonstrates that strategic blending of WFS and BA can maximize concrete strength while promoting sustainable use of industrial waste materials [53]. Further numerical modeling could support predictive mix design and broader application of these findings across variable cement types and curing conditions. The experimental outcomes obtained in this study are constructive compared to recent advancements in waste-based concrete development (Table 3).

Hence, the proposed mix design offers a practical, low-carbon alternative that aligns with ongoing global trends in sustainable concrete development. The combined use of WFS and BA at optimal levels was found to enhance both strength and durability parameters. While WFS alone showed limitations at higher contents due to increased water demand and poor workability, these effects were mitigated when combined with BA, which improved particle packing, reduced permeability, and contributed secondary pozzolanic activity. Thus, the 20% WFS + 20% BA blend emerged as the most effective mix in terms of performance balance, demonstrating improvements of 7.8% in compressive strength, 18.2% in chloride resistance, and 14.5% reduction in drying shrinkage.

Figure 14 shows a radar chart comparing six performance indicators across the control mix, WFS 20%, BA 20%, and the optimal binary blend (WFS + BA 20%). The WFS+BA 20% mix consistently outperforms all others across all parameters, demonstrating its superior material synergy. Compressive strength shows a 7.8% increase compared to the control. Similarly, split tensile and flexural strengths improved by 7.5% and 7.7%, respectively, due to better crack-bridging capability and a more cohesive matrix. Chloride resistance saw the highest gain—18.2% lower permeability—thanks to the refined pore structure formed by the combined filler effects of WFS and BA. Shrinkage was reduced by 14.5%, indicating enhanced internal curing and restrained

Table 3: Comparative analysis of related studies on waste valorization in concrete.

MATERIALS USED	KEY FINDINGS	COMPARISON WITH PRESENT STUDY
Fly ash, egg shell powder, steel fibers	Reduced water absorption and porosity; strength increased with triple blend	Comparable water absorption trend; your 20% WFS + 20% BA reduced absorption by 16.3% without steel fibers [54]
Mix	Optimum strength at 9% WGP + 1% RSF	Similar strength gain (7.8%) achieved without fibers; simpler and more economical mix [55]
Fly ash + metakaolin	Reduced drying shrinkage and crack formation	Drying shrinkage reduced by 14.5% in your study using WFS + BA alone [56]
FA + MK + 4 types of steel fibers	Hooked fibers enhanced performance most effectively	Strength enhancement achieved in your study without external fiber reinforcement [57]
FA + SF + steel fibers	Compressive, flexural, and tensile strength increased with triple blend	Comparable flexural (+7.7%) and tensile (+7.5%) gain achieved using dual waste sand replacement [58]
Alkali-activated slag concrete	AASC showed better mechanical properties at elevated temperatures	Your study complements AASC under ambient conditions with industrial sand substitutes [59]
Support Vector Machine (SVM) modeling for sediment transport	AI-based prediction for hydrological systems	Not directly relevant; no AI model used in this study, but experimental results show strong statistical correlation via RSM [60]

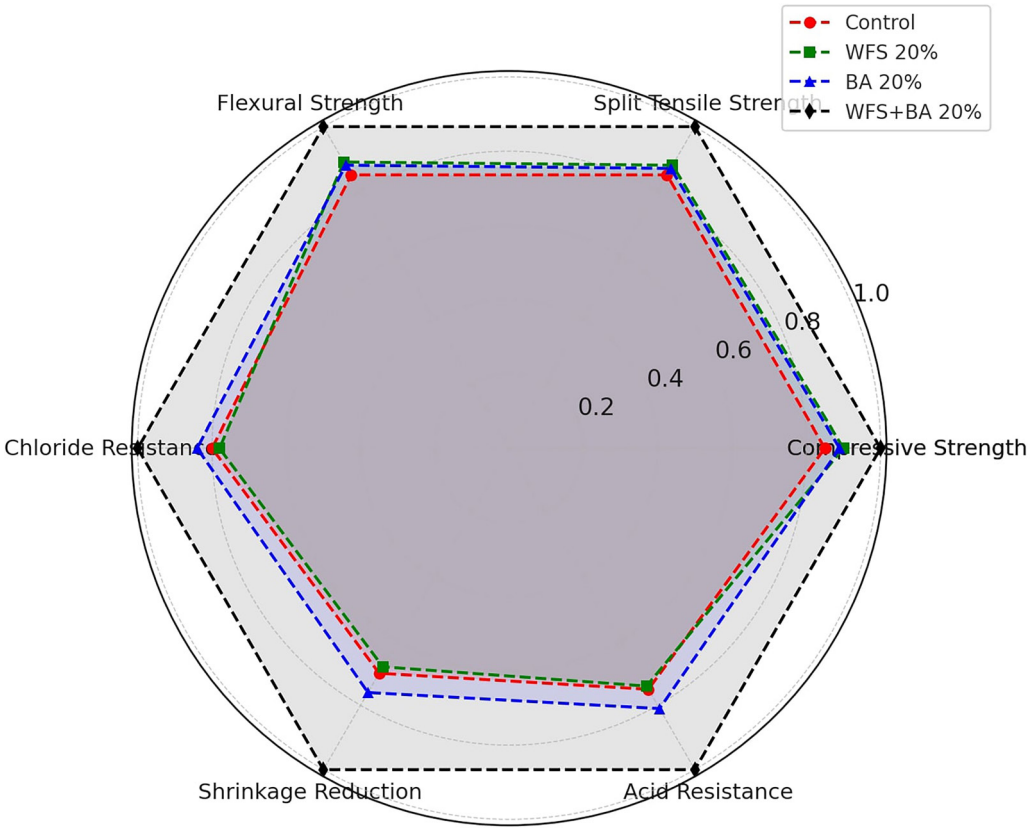

Figure 14: Radar chart illustrating the comparative performance of control.

moisture movement. This performance was better than both WFS 20% and BA 20% individually, which showed improvements of 5–10% across most parameters. The acid resistance of the WFS + BA blend improved by 11.2%, as the pozzolanic reaction reduced calcium hydroxide content, limiting acid attack susceptibility. In contrast, the WFS 20% mix underperformed in shrinkage resistance (lowest among the group), possibly due to its rough texture and increased water demand. BA 20% performed better than WFS 20% in durability metrics

but lagged in strength. The combined use of WFS and BA neutralized each other's limitations—namely, the angularity of WFS and the porosity of BA—resulting in an optimized matrix. The radar chart visually confirms that dual replacement offers a well-rounded enhancement across strength and durability parameters.

The proposed approach of using WFS and BA as partial replacements for fine aggregate offers several advantages. It enables the valorization of industrial byproducts, thus reducing environmental load and promoting circular economy practices. The 20% WFS + 20% BA combination significantly enhanced compressive, tensile, and flexural strengths while also reducing permeability, shrinkage, and acid attack—demonstrating excellent mechanical and durability performance without the need for additional chemical admixtures or fibers. Moreover, the approach remains cost-effective and aligns with sustainable construction goals. However, certain limitations were observed. The workability of WFS-dominant mixes decreased due to their high surface area and angular texture, requiring careful control of water content. Additionally, the study was conducted under controlled laboratory conditions, and the results may vary in field-scale applications or under harsh climatic conditions. Microstructural variability and potential long-term degradation behavior also require further exploration. Despite these limitations, the model presents a robust and replicable framework for eco-efficient concrete mix design.

4. CONCLUSIONS

The present investigation has demonstrated that integrating WFS and BA as partial replacements for fine aggregate in concrete can significantly enhance both mechanical performance and durability characteristics, provided the proportions are optimally balanced. The observed improvements in compressive strength, tensile capacity, and chloride resistance suggest that these industrial byproducts not only function as effective fillers but also contribute chemically through latent pozzolanic activity. Beyond performance enhancements, the findings underscore the potential of WFS and BA to promote sustainability in the construction sector by reducing reliance on natural sand and mitigating landfill waste. Importantly, the binary combinations of WFS and BA outperformed individual substitutions, revealing a synergistic interaction that improves microstructural density and durability. These insights position such blended mixes as viable alternatives for conventional concrete in both structural and exposure-prone environments. Future research should further explore the long-term performance under varied curing regimes and environmental stressors and investigate their compatibility with supplementary cementitious materials and chemical admixtures to advance the goal of greener and more resilient infrastructure.

In future investigations, the long-term performance of WFS and BA blended concrete under real environmental exposure may be examined. Additionally, LCA and embodied energy analysis may be conducted to evaluate economic feasibility of large-scale implementation. Microstructural modeling and simulation tools, including FEA, may be applied to predict damage propagation and service life performance. Furthermore, the influence of these waste materials on rheology, setting time, and shrinkage-induced cracking in high-performance and self-compacting concretes could be studied to broaden practical applications.

5. REFERENCES

[1] MALAIŠKIENĖ, J., VAIČIENĖ, M., "The influence of silica fly ash and wood bottom ash on cement hydration and durability of concrete", *Materials*, v. 17, n. 16, pp. 4031, 2024. http://doi.org/10.3390/ma17164031. PubMed PMID: 39203209.

[2] BURITATUM, A., SUDDEEPONG, A., HORPIBULSUK, S., *et al.*, "Improved performance of asphalt concretes using bottom ash as an alternative aggregate", *Sustainability*, v. 14, n. 12, pp. 7033, 2022. http://doi.org/10.3390/su14127033.

[3] RAHMAN, N.A., YIN, L.G., GUNESEGERAN, K., *et al.*, "Effectiveness of bottom ash as fine aggregate replacement in engineered cementitious composites", *Journal of Engineering Science and Technology*, v. 18, pp. 66–74, 2023.

[4] TORKITTIKUL, P., NOCHAIYA, T., WONGKEO, W., *et al.*, "Utilization of coal bottom ash to improve thermal insulation of construction material", *Journal of Material Cycles and Waste Management*, v. 19, n. 1, pp. 305–317, 2017. http://doi.org/10.1007/s10163-015-0419-2.

[5] ANEJA, S., SHARMA, A., GUPTA, R., *et al.*, "Bayesian regularized artificial neural network model to predict strength characteristics of fly-ash and bottom-ash based geopolymer concrete", *Materials*, v. 14, n. 7, pp. 1729, 2021. http://doi.org/10.3390/ma14071729. PubMed PMID: 33915938.

[6] ANKUR, N., SINGH, N., "Valorisation of bottom ash in concrete: serviceability, microstructural and sustainability characterisation", *Magazine of Concrete Research*, v. 76, n. 21, pp. 1241–1265, 2024. http://doi.org/10.1680/jmacr.23.00313.

[7] DONG, Y., XIANG, Y., HOU, H., *et al.*, "Remediation of Pb–Cd contaminated soil using coal bottom ash-based geopolymer and coir: soil remodeling and mechanism", *Journal of Cleaner Production*, v. 423, pp. 138706, 2023. http://doi.org/10.1016/j.jclepro.2023.138706.

[8] JAWAHAR, S., MAGESH, M., JAGEN, V., "Performance evaluation of concrete using bottom ash as fine aggregate", *International Journal of Innovative Technology and Exploring Engineering*, v. 8, pp. 95–100, 2019.

[9] MAGESH, M., JAWAHAR, S., DHANESH, E., *et al.*, "Influence of bottom ash as fine aggregate in ggbfs geopolymer concrete", *International Journal of Innovative Technology and Exploring Engineering*, v. 8, pp. 919–924, 2019.

[10] MENDA, S., POUDEL, S., USELDINGER-HOEFS, J., *et al.*, "Determining optimum coal bottom ash/slag content for sustainable concrete infrastructure", *Sustainability*, v. 17, n. 4, pp. 1429, 2025. http://doi.org/10.3390/su17041429.

[11] RAFIEIZONOOZ, M., KHANKHAJE, E., REZANIA, S., "Assessment of environmental and chemical properties of coal ashes including fly ash and bottom ash, and coal ash concrete", *Journal of Building Engineering*, v. 49, pp. 104040, 2022. http://doi.org/10.1016/j.jobe.2022.104040.

[12] SABARINATHAN, K., ARUNKUMAR, G., "Characterization study on concrete developed with fly ash, bottom ash, GGBS and construction debris", *Journal of Ceramic Processing Research*, v. 24, pp. 390–396, 2023. http://doi.org/10.36410/jcpr.2023.24.2.390.

[13] SINGH, D., SINGH, J., SINGH, J., "Sustainable management of sugarcane bagasse ash and coal bottom ash in concrete", *Nature Environment and Pollution Technology*, v. 16, pp. 295–300, 2017.

[14] VIRENDRA KUMARA, K.N., ANADINNI, S.B., "Influence of fly ash and bottom ash on properties of glass and polypropylene fiber reinforced concrete", *Indian Concrete Journal*, v. 92, pp. 50–56, 2018.

[15] PANDA, S., PRADHAN, M., PANIGRAHI, S.K., "Comparative study of opc and ppc-based concrete properties containing bottom ash and fly ash as fine aggregate", *Indian Concrete Journal*, v. 98, pp. 7–19, 2024.

[16] YAO, Y., ZHOU, L., HUANG, H., *et al.*, "Cyclic performance of novel composite beam-to-column connections with reduced beam section fuse elements", *Structures*, v. 50, pp. 842–858, 2023. http://doi.org/10.1016/j.istruc.2023.02.054.

[17] SUN, L., WANG, C., ZHANG, C., *et al.*, "Experimental investigation on the bond performance of sea sand coral concrete with FRP bar reinforcement for marine environments", *Advances in Structural Engineering*, v. 26, n. 3, pp. 533–546, 2023. http://doi.org/10.1177/13694332221131153.

[18] HUANG, H., GUO, M., ZHANG, W., *et al.*, "Seismic behavior of strengthened RC columns under combined loadings", *Journal of Bridge Engineering*, v. 27, n. 6, pp. 05022005, 2022. http://doi.org/10.1061/(ASCE)BE.1943-5592.0001871.

[19] NIU, Y., WANG, W., SU, Y., *et al.*, "Plastic damage prediction of concrete under compression based on deep learning", *Acta Mechanica*, v. 235, n. 1, pp. 255–266, 2024. http://doi.org/10.1007/s00707-023-03743-8.

[20] ZHANG, W., LIU, X., HUANG, Y., *et al.*, "Reliability-based analysis of the flexural strength of concrete beams reinforced with hybrid BFRP and steel rebars", *Archives of Civil and Mechanical Engineering*, v. 22, n. 4, pp. 171, 2022. http://doi.org/10.1007/s43452-022-00493-7.

[21] ZHANG, W., YANG, X., LIN, J., *et al.*, "Experimental and numerical study on the torsional behavior of rectangular hollow reinforced concrete columns strengthened By CFRP", *Structures*, v. 70, pp. 107690, 2024. http://doi.org/10.1016/j.istruc.2024.107690.

[22] LONG, X., MAO, M., SU, T., *et al.*, "Machine learning method to predict dynamic compressive response of concrete-like material at high strain rates", *Defence Technology*, v. 23, pp. 100–111, 2023. http://doi.org/10.1016/j.dt.2022.02.003.

[23] HUANG, Z., LUO, Y., ZHANG, W., *et al.*, "Thermal insulation and high-temperature resistant cement-based materials with different pore structure characteristics: performance and high-temperature testing", *Journal of Building Engineering*, v. 101, pp. 111839, 2025. http://doi.org/10.1016/j.jobe.2025.111839.

[24] ZHU, J.F., WANG, Z.Q., TAO, Y.L., *et al.*, "Macro–micro investigation on stabilization sludge as subgrade filler by the ternary blending of steel slag and fly ash and calcium carbide residue", *Journal of Cleaner Production*, v. 447, pp. 141496, 2024. http://doi.org/10.1016/j.jclepro.2024.141496.

[25] CUI, X., LIU, Y., DU, X., *et al.*, "Effect of fault dislocation on the deformation and damage behavior of ballastless track structures in tunnels", *Transportation Geotechnics*, v. 52, pp. 101561, 2025. http://doi.org/10.1016/j.trgeo.2025.101561.

[26] SINGH, M., SIDDIQUE, R., "Properties of concrete containing high volumes of coal bottom ash as fine aggregate", *Journal of Cleaner Production*, v. 91, pp. 269–278, 2015. http://doi.org/10.1016/j.jclepro.2014.12.026.

[27] IBRAHIM, M.H.W., ABIDIN, N.E.Z., JAMALUDDIN, N., *et al.*, "Bottom ash - potential use in self-compacting concrete as fine aggregate", *Journal of Engineering and Applied Sciences*, v. 11, pp. 2570–2575, 2016.

[28] ABBASS, M., AKHAI, S., "Exploring the sustainability potential of geopolymer concrete with coal bottom ash and basalt fibres", *Multiscale and Multidisciplinary Modeling, Experiments and Design*, v. 8, 2025. http://doi.org/10.1007/s41939-025-00794-3.

[29] DASH, M.K., PATRO, S.K., RATH, A.K., "Sustainable use of industrial-waste as partial replacement of fine aggregate for preparation of concrete: a review", *International Journal of Sustainable Built Environment*, v. 5, n. 2, pp. 484–516, 2016. http://doi.org/10.1016/j.ijsbe.2016.04.006.

[30] GILL, A.S., SIDDIQUE, R., "Durability properties of self-compacting concrete incorporating metakaolin and rice husk ash", *Construction & Building Materials*, v. 176, pp. 323–332, 2018. http://doi.org/10.1016/j.conbuildmat.2018.05.054.

[31] SALEH, F., GUNAWAN, M.A., YOLANDA, T.I., *et al.*, "Properties of mortar made with bottom ash and silica fume as sustainable construction materials", *World Journal of Engineering*, v. 20, n. 5, pp. 835–845, 2023. http://doi.org/10.1108/WJE-08-2021-0481.

[32] HAMADA, H., ALATTAR, A., TAYEH, B., *et al.*, "Sustainable application of coal bottom ash as fine aggregates in concrete: a comprehensive review", *Case Studies in Construction Materials*, v. 16, pp. e01109, 2022. http://doi.org/10.1016/j.cscm.2022.e01109.

[33] GURUMOORTHY, N., ARUNACHALAM, K., "Durability studies on concrete containing treated used foundry sand", *Construction & Building Materials*, v. 201, pp. 651–661, 2019. http://doi.org/10.1016/j.conbuildmat.2019.01.014.

[34] SINGH, A., ZHOU, Y., GUPTA, V., *et al.*, "Sustainable use of different size fractions of municipal solid waste incinerator bottom ash and recycled fine aggregates in cement mortar", *Case Studies in Construction Materials*, v. 17, pp. e01434, 2022. http://doi.org/10.1016/j.cscm.2022.e01434.

[35] MARTINS, M.A.B., SILVA, L.R.R., KUFFNER, B.H.B., *et al.*, "Behavior of high strength self-compacting concrete with marble/granite processing waste and waste foundry exhaust sand, subjected to chemical attacks", *Construction & Building Materials*, v. 323, pp. 126492, 2022. http://doi.org/10.1016/j.conbuildmat.2022.126492.

[36] YANG, K.-H., HWANG, Y.-H., LEE, Y., *et al.*, "Feasibility test and evaluation models to develop sustainable insulation concrete using foam and bottom ash aggregates", *Construction & Building Materials*, v. 225, pp. 620–632, 2019. http://doi.org/10.1016/j.conbuildmat.2019.07.130.

[37] MARTINS, M.A., BARROS, R.M., SILVA, L.R.R., *et al.*, "Durability indicators of high-strength self-compacting concrete with marble and granite wastes and waste foundry exhaust sand using electrochemical tests", *Construction & Building Materials*, v. 317, pp. 125907, 2022. http://doi.org/10.1016/j.conbuildmat.2021.125907.

[38] KIM, Y.-M., KIM, K., LE, T.H.M., "Advancing sustainability and performance with crushed bottom ash as filler in polymer-modified asphalt concrete mixtures", *Polymers*, v. 16, n. 12, pp. 1683, 2024. http://doi.org/10.3390/polym16121683. PubMed PMID: 38932033.

[39] LU, J., YANG, X., LAI, Y., *et al.*, "Utilization of municipal solid waste incinerator bottom ash (MSWIBA) in concrete as partial replacement of fine aggregate", *Construction & Building Materials*, v. 414, pp. 134918, 2024. http://doi.org/10.1016/j.conbuildmat.2024.134918.

[40] GANESAN, H., SACHDEVA, A., PETROUNIAS, P., *et al.*, "Impact of fine slag aggregates on the final durability of coal bottom ash to produce sustainable concrete", *Sustainability*, v. 15, n. 7, pp. 6076, 2023. http://doi.org/10.3390/su15076076.

[41] VIJAYAN, D.S., LEMA ROSE, A., GOKULNATH, V., *et al.*, "Experimental studies on strength and durability of sustainable concrete using bottom ash by replacement of fine aggregate", *Journal of Green Engineering*, v. 10, pp. 6938–6949, 2020.

[42] BILIR, T., YÜKSEL, I., TOPCU, I.B., *et al.*, "Effects of bottom ash and granulated blast furnace slag as fine aggregate on abrasion resistance of concrete", *Science and Engineering of Composite Materials*, v. 24, n. 2, pp. 261–269, 2017. http://doi.org/10.1515/secm-2015-0101.

[43] HADDADIAN, A., ALENGARAM, U.J., ALNAHHAL, A.M., *et al.*, "Valorization of diverse sizes of coal bottom ash as fine aggregate in the performance of lightweight foamed concrete", *Journal of Civil Engineering and Management*, v. 28, n. 8, pp. 601–619, 2022. http://doi.org/10.3846/jcem.2022.16995.

[44] AGGARWAL, Y., SIDDIQUE, R., "Microstructure and properties of concrete using bottom ash and waste foundry sand as partial replacement of fine aggregates", *Construction & Building Materials*, v. 54, pp. 210–223, 2014. http://doi.org/10.1016/j.conbuildmat.2013.12.051.

[45] VIVEK, S.S., SEHGAL, R., *Reclaimed waste materials for sustainable pavement construction*, Boca Raton, CRC Press, 2025. http://doi.org/10.1201/9781003598220.

[46] LIU, J., WU, Y., CHENG, L., *et al.*, "Recycling of municipal solid waste incineration bottom ash (MSWIBA) particles into natural fine sands for sustainable engineering cementitious composites", *Construction & Building Materials*, v. 418, pp. 135500, 2024. http://doi.org/10.1016/j.conbuildmat.2024.135500.

[47] SINGH, P., DASH, H.K., SAMANTARAY, S., "Effect of silica fume on engineering properties of expansive soil", *Materials Today: Proceedings*, v. 33, pp. 5035–5040, 2020. http://doi.org/10.1016/j.matpr.2020.02.839.

[48] YANG, X., LU, J., WAN, X., *et al.*, "Mechanical and microstructural properties of municipal solid waste incinerator bottom ash (MSWIBA) concrete exposed to salt erosion and drying-wetting cycles", *Journal of Building Engineering*, v. 96, pp. 110482, 2024. http://doi.org/10.1016/j.jobe.2024.110482.

[49] ABDULLAH, M.J., BEDDU, S., MANAN, T.S.B.A., *et al.*, "The strength and thermal properties of concrete containing water absorptive aggregate from well-graded Bottom Ash (BA) as partial sand replacement", *Construction & Building Materials*, v. 339, 2022. http://doi.org/10.1016/j.conbuildmat.2022.127658.

[50] VAN DEN HEEDE, P., RINGOOT, N., BEIRNAERT, A., *et al.*, "Sustainable high quality recycling of aggregates from waste-to-energy, treated in awet bottom ash processing installation, for use in concrete products", *Materials*, v. 9, n. 1, pp. 9, 2016. http://doi.org/10.3390/ma9010009. PubMed PMID: 28787809.

[51] CHINDASIRIPHAN, P., MEENYUT, B., ORASUTTHIKUL, S., *et al.*, "Influences of high-volume coal bottom ash as cement and fine aggregate replacements on strength and heat evolution of eco-friendly high-strength concrete", *Journal of Building Engineering*, v. 65, pp. 105791, 2023. http://doi.org/10.1016/j.jobe.2022.105791.

[52] ZHANG, Z., GUO, F., GAO, J., *et al.*, "Seismic performance of an innovative prefabricated bridge pier using rapid hardening ultra-high performance concrete", *Structures*, v. 74, pp. 108558, 2025. http://doi.org/10.1016/j.istruc.2025.108558.

[53] GONG, B., LI, H., "A couple Voronoi-RBSM modeling strategy for RC structures", *Structural Engineering and Mechanics*, v. 91, pp. 239–250, 2024. http://doi.org/10.12989/sem.2024.91.3.239.

[54] KUMAR, M.H., MACHARYULU, I.S., RAY, T., *et al.*, "Effect of water absorption and curing period on strength and porosity of triple blended concrete", *Materials Today: Proceedings*, v. 43, pp. 2162–2169, 2021. http://doi.org/10.1016/j.matpr.2020.12.092.

[55] KUMAR, M.H., MAHANTA, N.R., SAMANTARAY, S., *et al.*, "Combined effect of waste glass powder and recycled steel fibers on mechanical behavior of concrete", *SN Appl Sci*, v. 3, pp. 1–18, 2021. http://doi.org/10.1007/S42452-021-04353-6/FIGURES/13.

[56] KUMAR, M.H., MOHANTA, N.R., PATEL, N., *et al.*, "Impact of fly ash and metakaoline on the crack resistance and shrinkage of concrete", *Indian Journal of Science and Technology*, v. 46, pp. 2011–2026, 2022. http://doi.org/10.1007/S40996-021-00748-Y/METRICS.

[57] KUMAR, M.H., SAIKRISHNAMACHARYULU, I., KUMAR, U., *et al.*, "Coupling effect of fly ash, metakaoline and different types of steel fibers on mechanical performance of concrete", *AIP Conference Proceedings*, v. 2417, pp. 020014, 2021. http://doi.org/10.1063/5.0072573.

[58] KUMAR, M.H., SAIKRISHNAMACHARYULU, I., MOHANTA, N.R., *et al.*, "Mechanical behaviour of high strength concrete modified with triple blend of fly ash, silica fume and steel fibers", *Materials Today: Proceedings*, v. 65, pp. 933–942, 2022. http://doi.org/10.1016/j.matpr.2022.03.528.

[59] RAY, T., RANJAN MOHANTA, N., HITESH KUMAR, M., *et al.*, "Study of effect of temperature on behavior of alkali activated slag concrete", *Materials Today: Proceedings*, v. 43, pp. 1352–1357, 2021. http://doi.org/10.1016/j.matpr.2020.09.169.

[60] SAMANTARAY, S., SAHOO, A., PAUL, S., *et al.*, "Prediction of bed-load sediment using newly developed support-vector machine techniques", *Journal of Irrigation and Drainage Engineering*, v. 148, n. 10, pp. 04022034, 2022. http://doi.org/10.1061/(ASCE)IR.1943-4774.0001689.